Original Research

Experimental Insights and DFT Study of Green Synthesized CdS Nanoparticles, a Sustainable Approach for Preservation of *Capsicum chinense* Jacq.

Uday Sankar Senapati [1,*], J. Saikia [1], N. Seth [2], R. Buragohain [2]

[1] Department of Physics, Handique Girls' College, Guwahati-781001, Assam, India.
[2] Advanced Level Institutional Biotech Hub, Handique Girls' College, Guwahati-781001, Assam, India.
* Correspondence: uday.senapati@hgcollege.edu.in

Received: December 3, 2025; Accepted: March 11, 2026

Abstract: This study presents a novel approach for synthesizing CdS nanoparticles by employing tea (*Camellia sinensis* L.) leaf catechins as a potent chelating agent. The production of spherical, cubic, and crystallite CdS nanoparticles was confirmed by XRD and HRTEM investigations. The existence of biomolecules that encapsulated and stabilized the CdS nanoparticles was verified by UPLC and FTIR analysis. These nanoparticles demonstrated antimicrobial activity against microorganisms isolated from spoiled *Capsicum chinense* Jacq. Additionally, the cytotoxic effect of CdS nanoparticles on HEK-293 normal kidney cells showed safe level of cytotoxicity. The theoretical investigation reveals a substantial interaction between CdS nanoparticles and the bio- constituents of tea. Therefore, due to their favorable biocompatibility, antimicrobial activity, and low cytotoxicity, the green synthesized CdS nanoparticles hold promise as a preservative to control microbial contamination of *Capsicum chinense* Jacq., thereby enhancing its shelf life.

Keywords: green synthesis; CdS nanoparticles; antimicrobial activity; cytotoxicity; DFT.

1. Introduction

In light of the shifting global environment, ensuring food and nutritional security of the world's growing population is a difficult and demanding task. Hence, cutting-edge technologies like biotechnology and nanotechnology are thought to be the ideal ways to handle this difficult task by boosting production and lowering post-harvest losses. In developing countries , up to 30% of horticulture crop products are lost due to microbiological spoilage and physiological processes [1]. The majority of bacteria that were initially discovered on entire fruit or vegetable surfaces are found in soil. Studies have demonstrated that using contaminated irrigation water can raise the frequency of harmful microorganisms from harvest [2].

Bhut Jolokia (*Capsicum chinense* Jacq.) popularly known as King Chilli is a significant chilli that is widely grown, particularly in the northeastern Indian states of Assam, Nagaland, Manipur, and Arunachal Pradesh. In addition to its enormous domestic market demand, Bhut Jolokia has excellent export potential [3]. According to earlier research, a variety of bacteria that have been discovered from *Capsicum chinense* Jacq. may be the result of soil contamination as well as surface damage such bruising, cracks, and punctures that provide opportunities for the establishment and proliferation of spoilage microbes [4]. These issues may result in losses after harvest.

However, this post-harvest loss can be significantly reduced to an extent of 5-10% by the application of antimicrobial nanomaterials, thereby saving huge amounts of nutritious foods. Cadmium sulfide (CdS) nanoparticles have found several uses in the biomedical area because of its consistent, exceptional luminescence, continuous excitation spectrum, and narrow emission bands.

Different physical and chemical techniques are employed to produce CdS nanoparticles, however, these techniques are costly, time-consuming, need many synthetic stages and hazardous chemicals. Therefore, alternative approaches are needed that utilize nonhazardous materials, while maintaining important properties such as size, physiochemical characteristics, low cytotoxicity and biocompatibility. In this context, biogenic synthesis using bio surfactants presents a promising approach. According to recent findings, plant extracts mediated CdS nanoparticles exhibit outstanding antibacterial action and can be less harmful, biocompatible, and economically viable [5].

In the present case, catechin extract from tea leaves (*Camellia sinensis* L.) was used to synthesize CdS nanoparticles. The young leaves of tea plants contain around 25-30% polyphenols [6]. The polyphenols in tea contain a large group of chemicals such as flavonols (known as catechins), flavanols, organic acids, anthocyanins and many others. Among these constituents, catechins contribute more than 80% to the total polyphenolic content [7]. Therefore, in this green synthesis of CdS nanoparticles, catechins were used as the polyphenol source. Polyphenols have been observed to function as reducing, capping, and stabilizing agents during the nanoparticle synthesis process [8].

The synthesized CdS nanoparticles were tested for antimicrobial activity against spoilage microorganism isolated from King Chilli and cytotoxicity effect against a normal HEK-293 human cell line.

2. Materials and methods

Analytical grade chemicals were purchased from Sigma-Aldrich chemicals Pvt Ltd. (Bangalore, India) and used without further purification. Cadmium Sulphate ($CdSO_4$) and Sodium Sulphate (Na_2S) were used respectively as Cd^{2+} and S^{2-} source and *Camellia Sinensis* L. was collected from Jorhat, Assam, India and used as plant material. The synthesis was carried out using double distilled water.

Twenty grams of dried tea leaves were infused in 200 ml boiling water for 5 min, after which the leaves were filtered out. The resulting infusion contained catechins along with other water-soluble compounds and pigments. To remove caffeine and other pigments, the infusion was extracted with dichloromethane. The aqueous layer, containing catechins, was then subjected to ethyl acetate extraction to obtain the catechin fraction. This extract was dried using a rotary evaporator to yield crude catechin. For the synthesis of CdS nanoparticles, equimolar solutions of $CdSO_4$ and Na_2S were prepared. 50 ml of Na_2S solution was added drop wise to an equal amount of $CdSO_4$ solution. 5 ml of catechin extract was added drop wise to this mixture at 70°C with constant stirring. To complete the reaction and produce CdS nano colloids, the resulting solution was left at room temperature for the whole night. These nano colloids were centrifuged at 2,000 rpm for 15 min. The final product was ground into fine powder after being dried for 2 h at 120°C.

X-ray diffraction pattern of the synthesized nanoparticles was recorded by X-ray diffractometer (Philips X' pert with CuKα radiation, Philips Analytical, Netherland) using a wavelength of 0.154 nm. Particle size and morphology of the nanoparticles were examined using a transmission electron microscope (JEOL JEM 2100, JEOL Ltd., Japan). The biomolecules present in the tea leaf extract were identified using FTIR (Perkin Elmer spectrum RXI FTIR system, Parkin Elmer, USA) and UPLC analysis (Dionex, Ultimate 3000 UPLC system, Thermo Fisher Scientific, USA).

The microbes were isolated from a spoiled *Capsicum chinense* Jacq. sample, as per the procedure reported by Hasan et al. [9]. 16srRNA sequencing and bioinformatics analysis of the isolated microorganisms was carried as reported by Senapati et al. [10]. The QIAGEN DNeasy Ultra Clean Microbial Kit (Cat. No. / ID: 12224–50) was used to extract DNA from the culture. 1.0% agarose gel was used to assess its quality. There was only one high-molecular-weight DNA band visible. Forward (27 F: AGAGTTTGATCCTGGCTCAG) and reverse (1492 R: CGGTTACCTTGTTACGACTT) primers were used to amplify a portion of the 16S rRNA gene. On an agarose gel, a single distinct 1500 bp

PCR amplicon band was seen. To get rid of impurities, the PCR amplicon was purified using the QIAGEN QIAquick PCR Purification Kit (Cat. No. / ID: 28104). The aforementioned primers were used in the forward and reverse DNA sequencing reaction of the PCR amplicon using the BDT v3.1 Cycle sequencing kit on an Applied Biosystems Mini Amp Plus Thermal cycler, and the results were examined using an ABI 3730xl Genetic Analyzer. The standard well-diffusion method was used to investigate the antibacterial activity of CdS nanoparticles against the isolated microorganisms.

Human embryonic kidney cells (HEK-293) were grown in Dulbecco's Modified Eagle Medium and then cultured within a humidified incubator set at 37°C and an atmosphere enriched with 5% CO_2. Cell viability analysis was conducted using the MTT (3-(4, 5-dimethylthiazol-2-yl)-2, 5-diphenyltetrazolium bromide) assay, following established protocols [11]. The percentage ratio of treated cell absorbance to untreated control cell absorbance was used to measure the cytotoxicity of the CdS nanoparticles. Figure 1 shows the symmetric representation of green synthesis steps of the CdS nanoparticles and their applications.

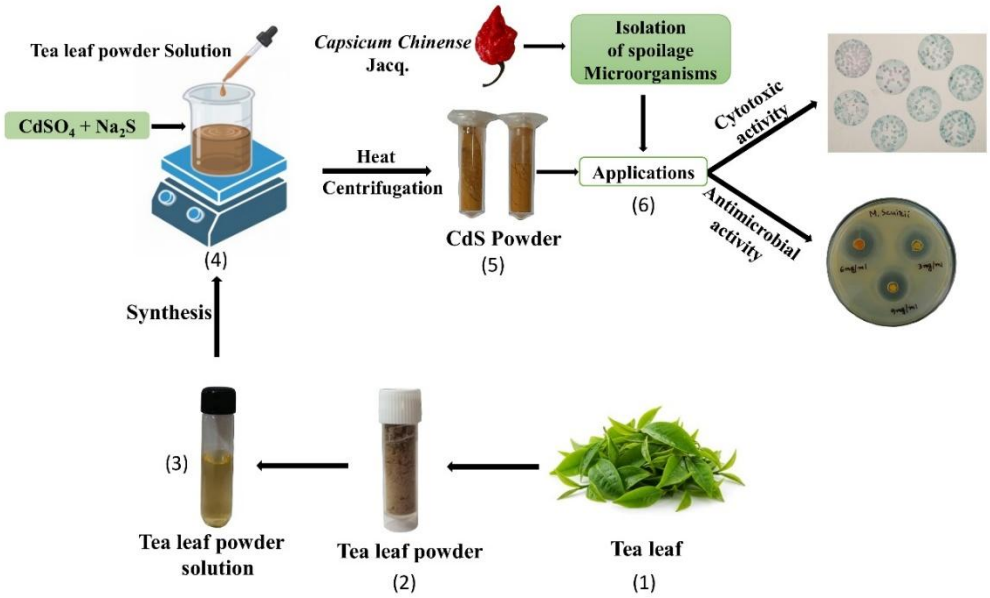

Figure 1. Symmetric representation of green synthesis steps of the CdS nanoparticles and their applications.

After processing fresh tea leaves (1) into dried tea leaf powder (2), the powder was removed to create a tea leaf powder solution (3). By reacting with $CdSO_4$ and Na_2S under carefully regulated heating and centrifugation, the extract served as a stabilizing and reducing agent for the production of CdS nanoparticles (4). A powder of the resultant CdS nanoparticles was collected (5). The produced CdS nanoparticles were then used for biological assessments, such as determining their cytotoxic activity against the HEK-293 kidney cell line and evaluating their antimicrobial activity against isolated spoilage microorganisms from *Capsicum chinense* Jacq. (6), indicating their potential use in food safety and preservation investigations.

3. Results and discussion

3.1. XRD, TEM and SAED analysis

The XRD patterns (Figure 2(a)) of CdS nanoparticles showed three peaks, each representing a distinct lattice plane at 2θ values of 26.67° (111), 43.93° (220), and 52.04° (311); these peaks are indicative of the cubic crystal structure of CdS (JCPDS10-0454). The average crystallite size of the CdS nanoparticles was estimated to be 2.47 nm using Debye Scherrer formula [12]. In case of green

synthesized CdS nanoparticles, the crystallite size found in the present study is smaller than that of Jarhad et al. [12] and Naranthatta et al. [13]. TEM analysis revealed that the size of the CdS nanoparticles varied from 2 to 8 nm (Figure 2(b)). The particles formed in different sizes indicated that the catechin extract might create polydisperse nanoparticles. The SAED pattern (Figure 2(c)) demonstrated the crystalline character of CdS nanoparticles where the diffraction rings correspond to (111), (220), and (311) planes, respectively. The data obtained from SAED is substantiated by the XRD results.

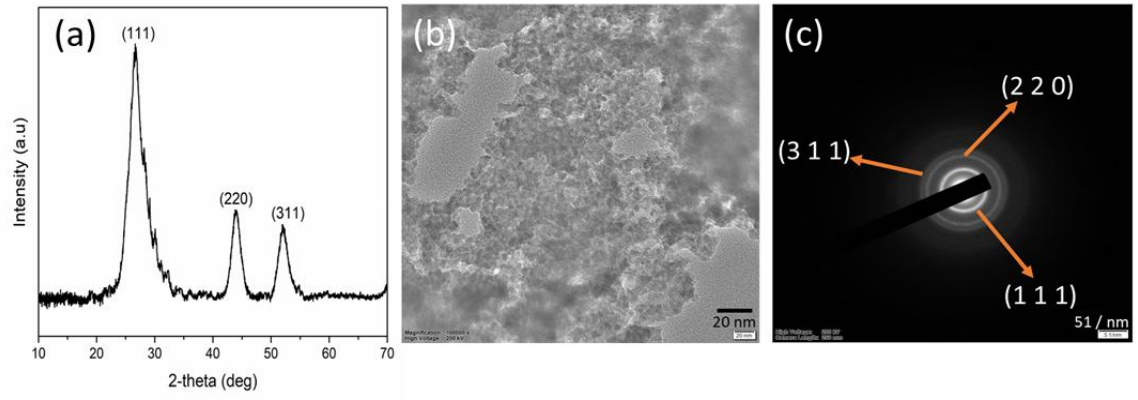

Figure 2. (a) XRD pattern, (b) TEM image and (c) SAED pattern of CdS nanoparticles.

3.2. UPLC and FTIR analysis

UPLC analysis of the catechin extract revealed the presence of five principal catechins namely (-) epigallocatechin-3-gallate (EGCG), (-) epigallocatechin (EGC), (-) epicatechin-3-gallate (ECG), (-) epicatechin (EC) and (+) catechin (Figure 3(b)). The content of EGCG, EGC, ECG, EC and +C catechin in the extract was found to be 29.49, 10.81, 11.89, 7.13 and 0.72 % respectively. Figure 3(a) shows the FTIR spectrum of catechin functionalized CdS nanoparticles. The stretching vibration of the O-H bond, the C=C group of the benzene ring, and the C-C stretching vibration of the catechin derivatives are identified as the absorption peaks at 3249 cm^{-1}, 1627 cm^{-1}, and 1105 cm^{-1}, respectively [14], which are displayed in scheme 1[15]. The peak that emerged in the fingerprint region at 616 cm^{-1} is associated with the Cd-S bond stretching mode of CdS [16]. FTIR analysis proves that the formation and stabilization of CdS nanoparticles are due to an interaction between the functional groups of the chemical constituents of catechin and metal ions.

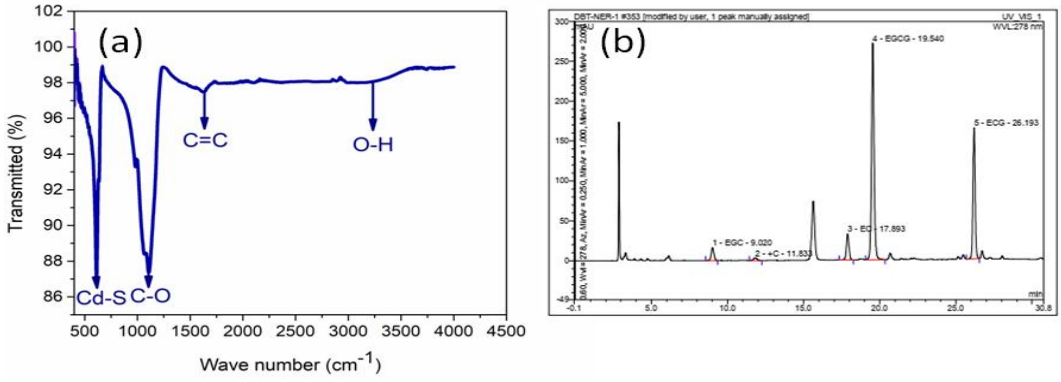

Figure 3. (a) FTIR spectrum of CdS nanoparticles and (b) UPLC spectrum of catechin extract.

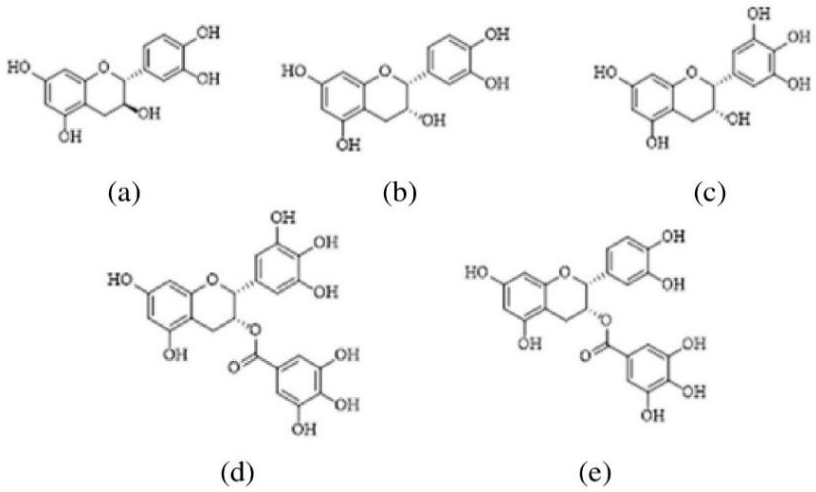

Scheme 1. Chemical structure of catechins: (a) (+)-catechin (+C); (b) (-)-epicatechin (EC); (c) (-)-epigallocatechin (EGC); (d) (-)-epigallocatechin gallate (EGCG); and (e) (-)-epicatechin gallate (ECG).

3.3. Identification of microorganisms

The 16s rRNA sequencing and bioinformatics analysis revealed the identities of the isolates to be *Mammaliicoccus sciuri*, *Paenibacillus sp.*, *Bacillus altitudinis* - the Gram- positive isolates and *Enterobacter sp*. - the Gram- negative isolate (Table 1).

Table 1. Results of 16s rRNA sequencing of the isolates.

Sample	Isolates	Colony Morphology	16S rRNA sequencing
***Capsicum chinense* Jacq.**	C1	Creamish, opaque, circular, muccoid, entire, flat mediumsized colony	*Mammalicoccus sciuri*
	C2	Yellowish, opaque, circular, muccoid, flat medium-sized colony	*Enterobacter sp.*
	C3	Creamish, opaque, irregular, dry, smooth, flat large-sized colony	*Bacillus altitudinis*
	C4	Whitish, transparent, circular, mucoid, flat large-sized colony.	*Paenibacillus sp.*

3.4. Antibacterial and cytotoxicity activity

The antibacterial activity of CdS nanoparticles was tested against three-gram positive bacteria *Mammaliicoccus sciuri*, *Paenibacillus sp.*, *Bacillus altitudinis* and one-gram negative bacteria *Enterobacter sp*. that were isolated from spoiled *Capsicum chinense* Jacq. The green synthesized CdS nanoparticles were found to have antibacterial activity against both gram-positive and gram-negative bacteria. (Figure 4 (a-d)). An appreciable increase was observed in the diameter of the inhibition zones with increase in the nanoparticle concentration (Table 2), showcasing a dose-dependent antibacterial

response. A large number of nanoparticles (at higher concentrations) interact with the bacterial cells strengthening the surface and electrical interactions which in turn increases the reactivity and antimicrobial efficiency of nanoparticles.

The comparative analysis demonstrated that the synthesized CdS NPs were more effective against Gram-positive bacteria compared to Gram-negative bacteria (Table 2) [17]. This variation in susceptibility is primarily due to difference in the cell wall architecture. Gram-negative bacteria possess an outer membrane additionally, which is rich in lipopolysaccharides and porin proteins acting as a selective permeability barrier and restricts the entry of antimicrobial agents. Conversely, Gram-positive bacteria lack this outer membrane and possess thick peptidoglycan layers embedded with teichoic acids which are negatively charged, and promoting intense electrostatic interaction with the CdS NPs [18] which are positively charged. Such interactions may result in the destabilization and disruption of the bacterial cell wall [19, 2].

Table 2. Zone of inhibition of isolates at different concentrations of CdS nanoparticles.

Microorganism	Concentration of CdS NPs and zone of inhibition (mm)		
	3 μg/ml	6 μg/ml	9 μg/ml
Mammaliicoccus sciuri	17	18	22
Bacillus altitudinis	27	30	31
Paenibacillus sp.	18	19	21
Enterobacter sp.	10	13	14

Concentration-dependent cell survival of HEK-293 kidney cell line was determined. The results showed that the CdS nanoparticles did not significantly affect the cell viability of HEK-293 kidney cells up to 10 μg/ml concentration and showed less than 2% inhibition (Figure 4(e)). The decline in cell viability could be the CdS nanoparticles' ability to produce reactive oxygen species that subsequently leads to the cell death.

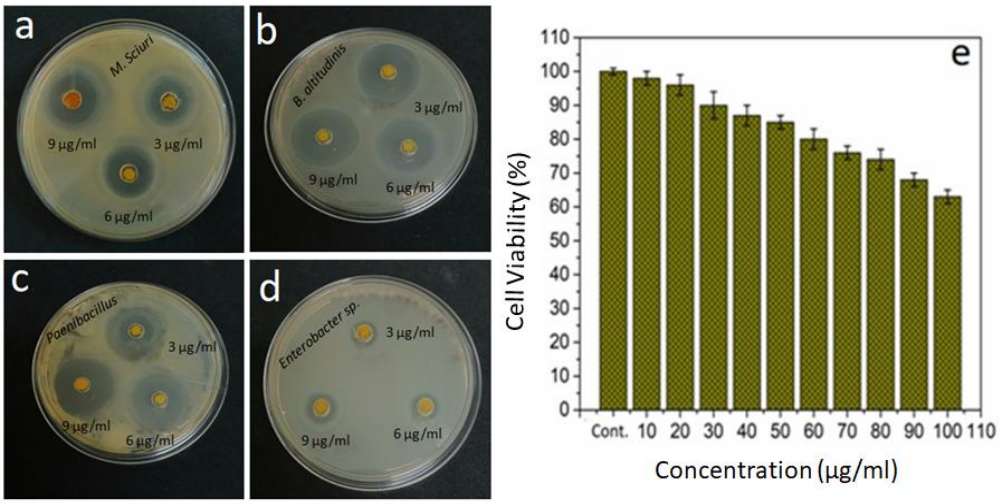

Figure 4. Antibacterial activity of CdS nanoparticles against (a) *Mammaliicoccus sciuri*, (b) *Bacillus altitudinis*, (c) *Paenibacillus sp.*, (d) *Enterobacter sp.* at different concentrations (3 μg/ml, 6 μg/ml and 9 μg/ml) and (e) cell viability of CdS nanoparticles using HEK-293 normal kidney cells.

3.5. Proposed mechanism of antibacterial activity of CdS NPs

Nanoparticles have gained much attention as antimicrobial agents, especially in combating the problem of microbial resistance [21]. Their nanoscale size provides a high surface-area-to-volume ratio, allowing increased contact with bacterial cells [22] and stronger antimicrobial activity.

In Gram-positive bacteria, the negatively charged teichoic acids present on the cell wall interact with cadmium of CdS NPs which ruptures the cell wall. Upon attachment and penetration of the CdS NPs, they induce reactive oxygen species (ROS) generation leading to oxidative stress which in turn compromises the cellular integrity by disrupting the cell structure and function [23]. The CdS NPs also have enhanced contact with thiol groups of significant respiratory enzymes of bacteria, leading to electron transport chain inhibition and cellular respiration impairment. In addition, nanoparticles bind to the enzymes present in the cell suppressing the activity of enzymes, interfering with the metabolic pathways in the cell, thus inhibiting DNA, RNA and protein synthesis [24]. Furthermore, the CdS NPs also promote ribosomal dissociation resulting in disruption of protein translation [25]. The cumulative effects of damage of the membrane, oxidative stress, inhibition of enzymes and macromolecule degradation finally leads to the loss of viability of cell and lysis of bacterial cell. An overview of the mechanisms of antibacterial activity of CdS NPs is shown in Figure 5.

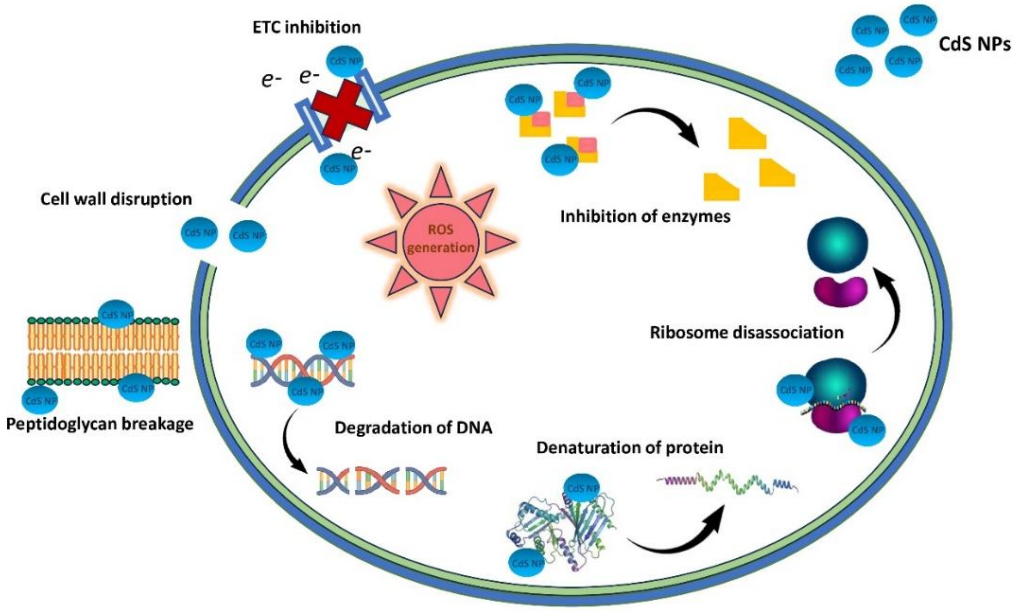

Figure 5. Summary of the effective mechanisms involved in the antibacterial activity of CdS nanopartricles.

3.6. Computational studies

To have a deeper insight into the interaction of CdS nanoparticles with the components present in tea, we carried out an intermolecular interaction study under DFT by employing B3LYP in conjunction with LANL2DZ level. The Becke's exchange three-parameter and Lee−Yang−Parr is a popular hybrid functional widely employed to study metal-ligand binding [26]. Literature available on the use of B3LYP/LANL2DZ functional in the study of cadmium coordination systems yields stable geometry configurations and consistency with the experimental results [27, 28].

We have chosen five major catechins, namely (+)-catechin (C), (−)-epicatechin (EC), (−)-epigallocatechin (EGC), (−)-epicatechin gallate (ECG), and (−)-epigallocatechin gallate (EGCG) present in tea [15]. Figure 6(a-e) show the proposed optimized structures of the interacting state of CdS nanoparticle (linear shape) with five major catechins found in tea, (+)-catechin−CdS (C−CdS), (−)-epicatechin−CdS (EC−CdS), (−)-epigallocatechin−CdS (EGC−CdS), (−)-epicatechin gallate−CdS (ECG−CdS), (−)-epigallocatechin gallate−CdS (EGCG−CdS), respectively. The structures are optimized at B3LYP/LANL2DZ level under DFT using Gaussian09W package. All the structures are in minimum energy with no imaginary frequencies, corroborating stable binding configuration [29].

The computed output shows that all the five bio-components interact with Cd atom through oxygen atom of O−H group having intermolecular distances ranging from 1.39−1.47 Å [30,31]. Owing to the formation of intermolecular bonding between CdS and catechin constituents, the bond lengths are found to be changed as compared to their monomer units (Table 3) [32]. A noticeable increment in length (0.02 Å) is detected in case of C−O bond, which is associated with the dramatic reduction of vibrational wavenumber of the interacting state (1105 cm^{-1} in FTIR spectrum) as compared to the reported peak of pure catechin (1144 cm^{-1}) [15].

Table 3. Selected bond distances of monomers and the interacting states.

Compound	Bond	Distance (Å)	Bond	Distances (Å)	Bond	Distance (Å)
C−CdS	C19-O5	1.413	O5−H34	0.978	O5····Cd36	2.413
	C21-O6	1.412	O6−H35	0.978	O6····Cd36	2.421
C	C19-O5	1.398	O5−H34	0.979		
	C21-O6	1.397	O6−H35	0.979		
EC−CdS	C19-O5	1.409	O5−H34	0.978	O5····Cd36	2.426
	C21-O6	1.410	O6−H35	0.978	O6····Cd36	2.421
EC	C19-O5	1.395	O5−H34	0.979		
	C21-O6	1.395	O6−H35	0.979		
EGC−CdS	C21-O6	1.404	O6−H35	0.978	O6····Cd37	2.470
	C22-O7	1.404	O7−H36	0.983	O7····Cd37	2.402
EGC	C21-O6	1.394	O6−H35	0.979		
	C22-O7	1.387	O7−H36	0.982		
ECG−CdS	C28-O9	1.418	O9−H49	0.978	O9····Cd1	2.405
	C26-O7	1.416	O7−H48	0.979	O7····Cd1	2.393
ECG	C24-O5	1.395	O5−H46	0.979		
	C26-O7	1.395	O7−H47	0.979		
EGCG−CdS	C27-O8	1.404	O8−H48	0.982	O8····Cd52	2.401
	C26-O6	1.406	O6−H47	0.978	O6····Cd52	2.458
EGCG	C27-O8	1.388	O8−H48	0.983		
	C26-O6	1.395	O6−H47	0.979		

The binding energies are calculated as −31.68 kcal/mol, −28.92 kcal/mol, −29.36 kcal/mol, −42.48 kcal/mol, and −30.62 kcal/mol, respectively, for C−CdS, EC−CdS, EGC−CdS, ECG−CdS, and EGCG−CdS systems. The negative of the binding energy suggests a stable interaction between CdS nanoparticle and the selected catechin components present in tea [33].

To quantify the nature and strength of interaction between the catechin components and CdS nanoparticles, QTAIM (Quantum Theory of Atoms in Molecules) analysis is carried out at bond critical points (Table 4). All the topological parameters are calculated using Multiwfn software, which presents positive values for electron density ranging from 0.0313−0.0369 a.u. indicating ionic

interactions [34]. The positive Laplacian reveals electronic charge depletion through the bond path corresponding to electrostatic interaction [35,36]. Total energy density H(r)=Kinetic Energy G(r)+Potential Energy V(r) is positive for all the interacting states depicting destabilization of electron density and ionic characteristics [21]. The computed bond energy (E_{bond}= − V(r)/2 × 627.51 kcal/mol) increases or decreases according to the bond distance and is listed in Table 4.

Table 4. The electron density (ρ), Laplacian of electron density ($\nabla^2\rho$), energy density (H(r)), Lagrangian K.E. G(r), potential energy density V(r), bond energy E_{bond}, and bond distances at the bond critical points (BCPs) of the interacting states at B3LYP/LANL2DZ level using the AIM theory.

Compound	Intermolecular interactions	ρ_{BCPs} (a.u.)	$\nabla^2\rho_{BCPs}$ (a.u.)	H(r) (a.u.)	G(r) (a.u.)	V(r) (a.u.)	E_{bond} (kcal/mol)	Bond distance (Å)
C–CdS	O5····Cd36	0.0356	0.2063	0.0017	0.0444	−0.0436	13.67	2.413
	O6····Cd36	0.0349	0.2018	0.0019	0.0433	−0.0414	12.98	2.421
EC–CdS	O5····Cd36	0.0345	0.1991	0.0020	0.0427	−0.0407	12.76	2.426
	O6····Cd36	0.0345	0.1999	0.0020	0.0427	−0.0407	12.76	2.421
EGC–CdS	O6····Cd37	0.0313	0.1778	0.0027	0.0376	−0.0349	10.95	2.470
	O7····Cd37	0.0364	0.2110	0.0015	0.0456	−0.0441	13.83	2.402
ECG–CdS	O9····Cd1	0.0369	0.2102	0.0013	0.0455	−0.0441	13.83	2.405
	O7····Cd1	0.0383	0.2176	0.0010	0.0474	−0.0464	14.55	2.393
EGCG–CdS	O8····Cd52	0.0365	0.2118	0.0015	0.0458	−0.0442	13.86	2.401
	O6····Cd52	0.0321	0.1833	0.0025	0.0389	−0.0364	11.42	2.458

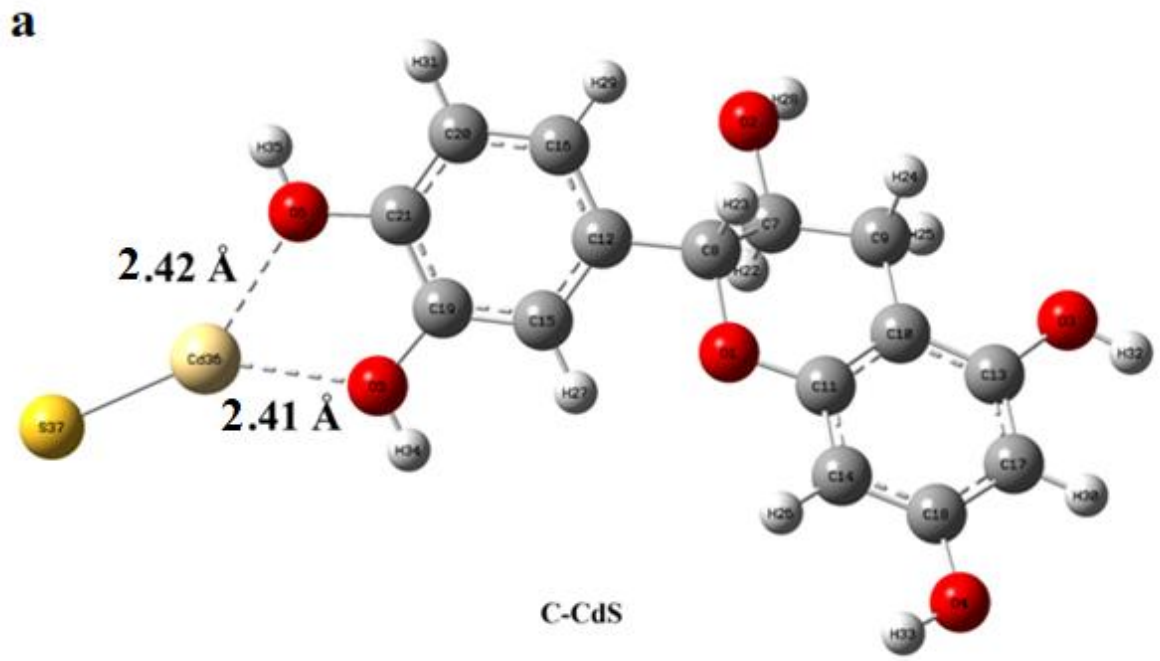

b

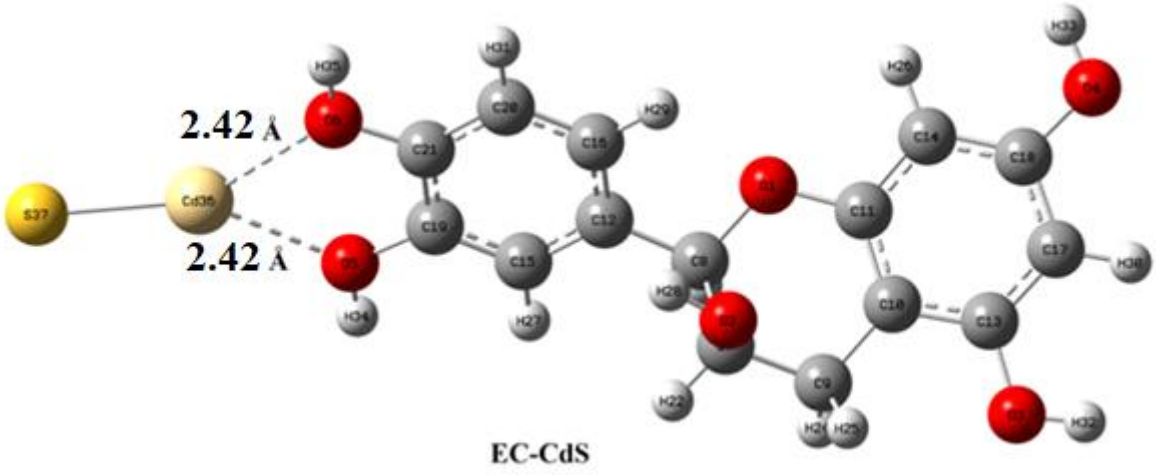

EC-CdS

c

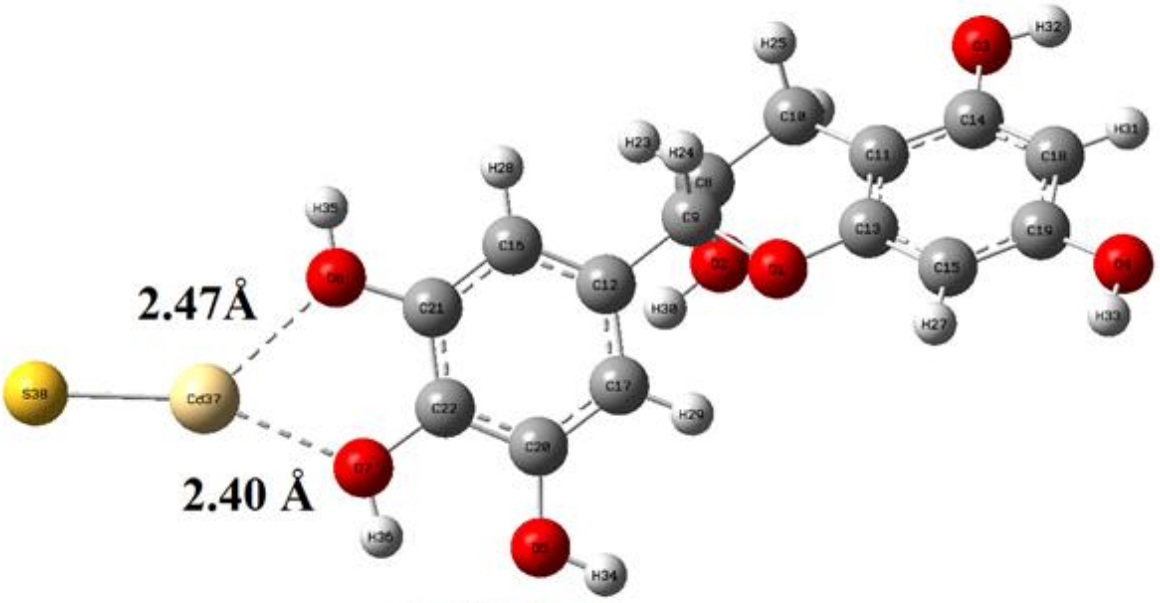

EGC-CdS

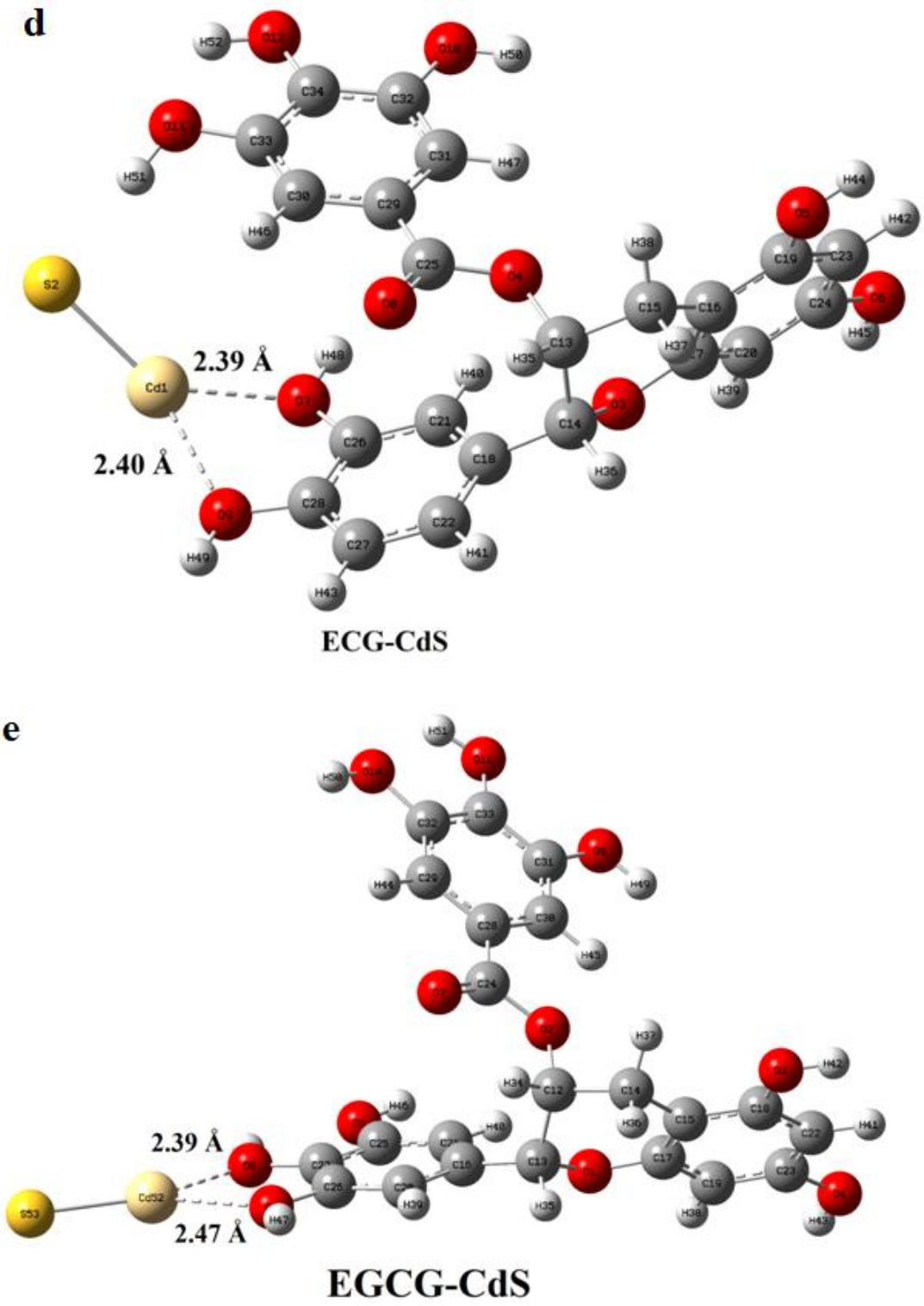

Figure 6. Optimized structures of the interacting state of CdS nanoparticle (linear shape) with five major catechins found in tea, namely (a) (+)-catechin−CdS (C−CdS), (b) (−)-epicatechin−CdS (EC−CdS), (c) (−)-epigallocatechin−CdS (EGC−CdS), (d) (−)-epicatechin gallate−CdS (ECG−CdS), (e) (−)-epigallocatechin gallate−CdS (EGCG−CdS).

Thus, catechin-mediated green synthesized CdS nanoparticles exhibited potential for usage as a preservative. Nevertheless, more investigation is required to fully grasp this potential.

4. Limitations

Despite being economical and environmentally benign, the green synthesis of CdS nanoparticles utilizing tea catechin has limitations with regard to reproducibility and exact control over particle size and morphology. Nanoparticle characteristics may vary from batch to batch due to variations in the plant extract's composition and catechin content. Organic capping compounds may occasionally lessen CdS nanoparticles' direct engagement with microbial cells in antibiofilm research, hence decreasing their effectiveness. Therefore, before considering their biological usage, meticulous optimization and a comprehensive toxicity evaluation are crucial.

5. Conclusion

For the first time, catechins extracted from tea leaves were used to synthesize CdS nanoparticles in an easy, economical, and environmentally benign method. From XRD analysis, it was found that the CdS nanoparticles had a cubic shape and an average crystallite size of 2.47 nm. The SAED results validate the XRD data. The size range of the CdS nanoparticles, according to TEM examination, was 2 to 8 nm. The biomolecules found in catechin extract were significant in keeping the CdS nanoparticles stable. The microorganisms isolated from spoiled *Capsicum chinense* Jacq. were effectively inhibited by the CdS nanoparticles. When applied to HEK-293 normal kidney cells, CdS nanoparticles had a minimal cytotoxic effect. As shown by theoretical study, there is a substantial electrostatic interaction between the bio- constituents of tea and CdS nanoparticles, which might enhance the stability of the CdS nanoparticles. The findings demonstrated that the catechins extract-mediated CdS nanoparticles are a potentially useful biomaterial for improving the shelf life of *Capsicum chinense* Jacq.

Availability of Data and Materials: The dataset on which the conclusion of this manuscript depends will be available to the readers on request.

Author Contributions: Uday Sankar Senapati-Methodology, formal analysis, writing and editing the manuscript; J. Saikia -Computational analysis, writing and editing the manuscript; N. Seth-Experimental assessment, writing and editing the manuscript; R. Buragohain- Experimental assessment, writing and editing the manuscript. All authors have read and approved the final manuscript. All authors contributed to editorial changes in the manuscript. All authors have participated sufficiently in the work and agreed to be accountable for all aspects of the work.

Acknowledgements: Authors acknowledge Advanced Level Institutional Biotech Hub, Handique Girls' College, Guwahati, Assam, India and Dr. H. Deka, Biochemistry Department, Tocklai Tea Research Institute, Jorhat, Assam, India respectively for providing laboratory facilities and catechin extraction from tea with UPLC characterization.

Funding: This research received no external funding.

Conflict of Interest: The authors declare no conflict of interest.

References

1. Amin, R.R.; Siddiqui, M.N.; Skalicky, M.; Brestic, M.; Hossain, A.; Kayesh, E. Prospects of nanotechnology in improving the productivity and quality of horticultural crops. *Horticulturae* 2021, 7(10), 332. https://doi.org/10.3390/horticulturae7100332

2. Barth, M.; Hankinson, T.R.; Zhuang, H.; Breidt, F. Microbiological spoilage of fruits and vegetables. In: *Compendium of the Microbiological Spoilage of Foods and Beverages*; Springer: New York, NY, USA, 2009; pp. 135-183. https://doi.org/10.1007/978-1-4419-0826-1_6

3. Das, A.; Das, D.; Munshi, S.A. Bhut Jolokia (King Chilli) husbandry: A potential entrepreneurial option in North-East India. *SSRN* 2024. https://dx.doi.org/10.2139/ssrn.4943602

4. Amruthraj, N.J.; Raj, J.P.P.; Lebel, A. Isolation and molecular characterization of plant growth promoting rhizobacterium *Paenibacillus illinoisensis* strain nagoth jar 007 from seeds of Capsicum chinensis Bhut Jolokia. *Journal of Microbiology, Biotechnology and Food Sciences* 2014, 3, 391-394. https://office2.jmbfs.org/index.php/JMBFS/article/view/7001

5. Shivaji, K.; Mani, S.; Ponmurugan, P.; De Castro, C.S.; Davies, M.L.; Balasubramanian, M.G. Green-synthesis-derived CdS quantum dots using tea leaf extract: antimicrobial, bioimaging, and therapeutic applications in lung cancer cells. *ACS Applied Nano Materials* 2018, 1(4), 1683-1693. https://doi.org/10.1021/acsanm.8b00147

6. Deka, H.; Sharmah, P.P.; Chowdhury, P.; Rajkhowa, K.; Sabhapondit, S.; Panja, S. Impact of the season on total polyphenol and antioxidant properties of tea cultivars of industrial importance in Northeast India. *Foods* 2023, 12, 3196. https://doi.org/10.3390/foods12173196

7. Deka, H.; Barman, T.; Dutta, J.; Devi, A.; Tamuly, P.; Paul, R.K. Catechin and caffeine content of tea (*Camellia sinensis L.*) leaf significantly differ with seasonal variation: a study on popular cultivars in North East India. *Journal of Food Composition and Analysis* 2021, 96, 103684. https://doi.org/10.1016/j.jfca.2020.103684

8. Nikam, S.A.; Chaudhari, S.P. Biosynthesis of silver nanoparticles from polyphenolic extract of Baliospermum solanifolium using central composite design. *Pharmacognosy Research* 2022, 14(4), 405-411. https://doi.org/10.5530/pres.14.4.59

9. Hasan, N.A.; Zulkahar, I.M. Isolation and identification of bacteria from spoiled fruits. *AIP Conference Proceedings* 2018, 2020, 020073. https://doi.org/10.1063/1.5062699

10. Senapati, U.S.; Chauhan, P.; Kalita, H.; Das, A.; Saikia, J.; Goswami, M.; et al. Green synthesis, characterization and bioactivity of zinc oxide nanoparticles: Experimental and computational approaches. *Next Nanotechnology* 2025, 7, 100194. https://doi.org/10.1016/j.nxnano.2025.100194

11. Saranya, S.; Vijayaranai, K.; Pavithra, S.; Raihana, N.; Kumanan, K. In vitro cytotoxicity of zinc oxide, iron oxide and copper nanopowders prepared by green synthesis. *Toxicology Reports* 2017, 4, 427-430. https://doi.org/10.1016/j.toxrep.2017.07.005

12. Jarhad, K.V.; Pawanoji, A.A.; Parab, P.S.; Pawar, A.S. Green synthesis of multifunctional CdS nanoparticles from cinnamon (Cinnamomum verum) extract: in vitro biomedical, photocatalytic degradation and photoelectrochemical applications. *BioNanoScience* 2025, 15, 155. https://doi.org/10.1007/s12668-024-01623-6

13. Naranthatta, S.; Janardhanan, P.; Pilankatta, R.; Nair, S.S. Green synthesis of engineered CdS nanoparticles with reduced cytotoxicity for enhanced bioimaging application. *ACS Omega* 2021, 6(12), 8646-8655. https://doi.org/10.1021/acsomega.1c00519

14. Zhao, B.; Deng, S.; Li, J.; Sun, C.; Fu, Y.; Liu, Z. Green synthesis, characterization and antibacterial study on catechin-functionalized ZnO nanoclusters. *Materials Research Express* 2021, 8(2), 025006. https://doi.org/10.1088/2053-1591/abe255

15. Deka H.; Sarmah P.P.; Devi A.; Tamuly P.; Karak T. Changes in major catechins, caffeine, and antioxidant activity during CTC processing of black tea from North East India. *RSC Advances* 2021, 11(19), 11457–11467. https://doi.org/10.1039/D0RA09529J

16. Kumar S.; Sharma J.K. Stable phase CdS nanoparticles for optoelectronics: a study on surface morphology, structural and optical characterization. *Materials Science-Poland* 2016, 34(2), 368-373. https://doi.org/10.1515/msp-2016-0033

17. Ghasempour, A.; Dehghan, H.; Ataee, M.; Chen, B.; Zhao, Z.; Sedighi, M.; Guo, X.; Shahbazi, M.A. Cadmium sulfide nanoparticles: preparation, characterization, and biomedical applications. *Molecules* 2023, 28(9), 3857. https://doi.org/10.3390/molecules28093857

18. Bhat, I.U.H.; Yi, Y.S. Green synthesis and antibacterial activity of cadmium sulfide nanoparticles (CdSNPs) using Panicum sarmentosum. *Asian Journal of Green Chemistry* 2019, 3(4), 455–469. https://doi.org/10.33945/SAMI/AJGC.2019.4.3

19. Alsaggaf, M.S.; Elbaz, A.F.; El Badawy, S.; Moussa, S.H. Anticancer and antibacterial activity of cadmium sulfide nanoparticles by Aspergillus niger. *Advances in Polymer Technology* 2020, 2020, 4909054. https://doi.org/10.1155/2020/4909054

20. Khane, Y.; Benouis, K.; Albukhaty, S.; Sulaiman, G.M.; Abomughaid, M.M.; Al Ali, A. Green synthesis of silver nanoparticles using aqueous Citrus limon zest extract: characterization and evaluation of their antioxidant and antimicrobial properties. *Nanomaterials* 2022, 12(12), 2013. https://doi.org/10.3390/nano12122013

21. León-Buitimea, A.; Garza-Cárdenas, C.R.; Garza-Cervantes, J.A.; Lerma-Escalera, J.A.; Morones-Ramírez, J.R. The demand for new antibiotics: antimicrobial peptides, nanoparticles, and combinatorial therapies as future strategies in antibacterial agent design. *Frontiers in Microbiology* 2020, 11, 1669. https://doi.org/10.3389/fmicb.2020.01669

22. Ahmed, F.; AlOmar, S.Y.; Albalawi, F.; Arshi, N.; Dwivedi, S.; Kumar, S. Microwave mediated fast synthesis of silver nanoparticles and investigation of their antibacterial activities for Gram-positive and Gram-negative microorganisms. *Crystals* 2021, 11(6), 666. https://doi.org/10.3390/cryst11060666

23. Regmi, A.; Basnet, Y.; Bhattarai, S.; Gautam, S.K. Cadmium sulfide nanoparticles: synthesis, characterization, and antimicrobial study. *Journal of Nanomaterials* 2023, 2023(1), 8187000. https://doi.org/10.1155/2023/8187000

24. Shivashankarappa, A.; Sanjay, K.R. *Escherichia coli*-based synthesis of cadmium sulfide nanoparticles: characterization, antimicrobial and cytotoxicity studies. *Brazilian Journal of Microbiology* 2020, 51(3), 939–948. https://doi.org/10.1007/s42770-020-00238-9

25. Durán, N.; Nakazato, G.; Seabra, A.B. Antimicrobial activity of biogenic silver nanoparticles and silver chloride nanoparticles: an overview and comments. *Applied Microbiology and Biotechnology* 2016, 100(15), 6555–6570. https://doi.org/10.1007/s00253-016-7657-7

26. Gallegos, F.E.; Meneses, L.M.; Cuesta, S.A.; Santos, J.C.; Arias, J.; Carrillo, P.; Pilaquinga, F. Computational modeling of the interaction of silver clusters with carbohydrates. *ACS Omega* 2022, 7(6), 4750-4756. https://pubs.acs.org/doi/10.1021/acsomega.1c04149

27. Demir, S.; Dikmen, G.; Erer, H. 2D Cadmium (II) Coordination Polymer Based on 2, 5-Furandicarboxylate and 1, 4-Bis (1 H-imidazol-1-yl) butane Linkers: Synthesis, Characterization and DFT Studies. *Journal of Inorganic and Organometallic Polymers and Materials* 2024, 34(9), 4203-4213. https://doi.org/10.1007/s10904-024-03083-7

28. Masoudiasl, A.; Montazerozohori, M.; Joohari, S.; Taghizadeh, L.; Mahmoudi, G.; Assoud, A. Structural investigation of a new cadmium coordination compound prepared by sonochemical process: Crystal structure, Hirshfeld surface, thermal, TD-DFT and NBO analyses. *Ultrasonics Sonochemistry* 2019, 52, 244-256. https://doi.org/10.1016/j.ultsonch.2018.11.024

29. Dong, S.; Jin, X.; Hou, X. Cluster-continuum calculations of coordination structures and formation constants for aqueous cadmium halide Complexes. *The Journal of Physical Chemistry A* 2025, 129(39), 8922-8934. https://doi.org/10.1021/acs.jpca.5c02260

30. Jalilehvand, F.; Mah, V.; Leung, B.O.; Mink, J.; Bernard, G.M.; Hajba, L. Cadmium (II) cysteine complexes in the solid state: a multispectroscopic study. *Inorganic Chemistry* 2009, 48, 4219-4230. https://doi.org/10.1021/ic900145n

31. Wang, X.F.; Bao, C.H.; Xia, S.S.; Cai, Y.; Wang, X.S.; Sun, J. Solvent-assisted synthesis and characterization of 2D and 3D cadmium metal–organic framework. *Structural Chemistry* 2025, 1-8. https://doi.org/10.1007/s11224-025-02532-4

32. Saikia, J.; Devi, T.G.; Karlo, T. Synthesis, spectroscopic, and molecular interaction study of lead (II) complex of DL-alanine using experimental techniques and quantum chemical calculations. *Journal of Molecular Structure* 2023, 1283, 135208. https://doi.org/10.1016/j.molstruc.2023.135208

33. Begum, T.; Agarwal, S.; Bhuyan, P.; Das, J.; Verma, A.K.; Guha A. *Aloe vera* gel mediated green synthesis of ruthenium nanoparticles and their potential anticancer activity. *Next Nanotechnology* 2025, 7, 100095. https://doi.org/10.1016/j.nxnano.2024.100095

34. Abdullah, N.A.F.; Hasan, S.; Lee, S.A. AIM and ELF bonding analyses of M–O and M–N (Metal= Ba, Y, Zr) in metal–complexes using DFT approach. *Science Letters (ScL)* 2021, 15(1), 90-100. https://doi.org/10.24191/sl.v15i1.11798

35. Soliman, S.M.; Albering, J.; Abu-Youssef, M.A.M. Structural analyses of two new highly distorted octahedral copper (II) complexes with quinoline-type ligands; Hirshfeld, AIM and NBO studies. *Polyhedron* 2017, 127, 36-50. https://doi.org/10.1016/j.poly.2017.01.051

36. Mary C.P.V.; Vijayakumar S.; Shankar R. Metal chelating ability and antiox- idant properties of Curcumin-metal complexes – a DFT approach. *Journal of Molecular Graphics and Modelling* 2018, 79, 1-14. https://doi.org/10.1016/j.jmgm.2017.10.022